ter at pH 2 to 4. These were titrated to pH ≥6 to generate precipitates. The solutions were agitated repeatedly over 2 to 240 hours, and the pH was adjusted to compensate for acidification from cation hydrolysis. Filtered aliquots of the solutions were spiked with a ^{191}Ir-enriched tracer and analyzed by isotope dilution inductively coupled plasma mass spectrometry (ICP-MS). Both Fe and Mn particles scavenged >50% of the Ir at alkaline pH, in both freshwater and seawater. Scavenging efficiency increased with increased pH, consistent with cation adsorption. Increased scavenging in freshwater probably reflects a shift in speciation from anionic chloro-complexes to hydroxy- and mixed hydroxy-chloro–complexes that are more readily scavenged.
20. D. C. Colodner, E. A. Boyle, J. M. Edmond, J. Thomson, *Nature* **358**, 402 (1992).
21. L. Zhou and F. T. Kyte, *Paleoceanography* **7**, 441 (1992); F. T. Kyte, K. Leinen, R. G. Heath, L. Zhou, *Geochim. Cosmochim. Acta* **57**, 1719 (1993).
22. M. C. Wells, P. N. Boothe, B. J. Presley, *Geochim. Cosmochim. Acta* **52**, 1737 (1988); J. Li and R. H. Byrne, *Environ. Sci. Tech.* **24**, 1038 (1990); S. A. Wood, *Can. Mineral.* **28**, 665 (1990); ______, C. D. Tait, D. Vlassopoulos, *Geochim. Cosmochim. Acta* **58**, 625 (1994).
23. D. W. Spencer and P. G. Brewer, *J. Geophys. Res.* **76**, 5877 (1971); S. Emerson, R. E. Cranston, P. S. Liss, *Deep-Sea Res.* **26A**, 859 (1979).
24. D. Dzombak and F. M. M. Morel, *Surface Complexation Modelling* (Wiley, New York, 1990); Y. Erel and J. J. Morgan, *Geochim. Cosmochim. Acta* **55**, 1807 (1991).
25. H. Gamsjäger and P. Beutler, *J. Chem. Soc. Dalton Trans.*, **1979**, 1415 (1979); C. F. Baes and R. E. Mesmer, *The Hydrolysis of Cations* (Krieger, Malabar, FL, 1986).
26. A global river water flux of 4.2 × 10^4 km^3 year^{-1} is used [M. I. Lvovitch, *Eos* **54**, 28 (1973)].
27. R. A. Duce *et al.*, *Global Biogeochem. Cycles* **5**, 193 (1991).
28. S. G. Love and D. E. Brownlee, *Science* **262**, 550 (1993).
29. B. K. Esser and K. K. Turekian, *Geochim. Cosmochim. Acta* **52**, 1383 (1988).
30. K. W. Bruland, in *Chemical Oceanography*, J. P. Riley and R. Chester, Eds. (Academic Press, London, 1983), vol. 8, pp. 157.
31. C. B. Officer, A. Hallam, C. L. Drake, J. D. Devine, *Nature* **326**, 143 (1987).
32. R. Rocchia *et al.*, *Earth Planet. Sci. Lett.* **99**, 206 (1990).
33. R. A. Creaser contributed to the development of the analytical methods. We thank D. Karl and others involved in the HOT program for help in sampling the Pacific Ocean, M. Roy-Barman and D. Porcelli for their assistance in the field, and G. Ravizza for his thoughtful comments. Supported by U.S. Department of Energy grant DE-FG03-88ER13851, NASA grant NAGW-3337, and by an NSF Graduate Research Fellowship to A.D.A. Ship time on the R.V. *Moana Wave* was supported by NSF OCE-9303094 (R. Lukas) and OCE-9301368 (D. Karl). Division contribution number 5669 (931).

26 April 1996; accepted 17 July 1996

Seismic Evidence for Partial Melt at the Base of Earth's Mantle

Quentin Williams* and Edward J. Garnero

The presence of an intermittent layer at the base of Earth's mantle with a maximum thickness near 40 kilometers and a compressional wave velocity depressed by ~10 percent compared with that of the overlying mantle is most simply explained as the result of partial melt at this depth. Both the sharp upper boundary of this layer (<10 kilometers wide) and the apparent correlation with deep mantle upwelling are consistent with the presence of liquid in the lowermost mantle, implying that the bottom of the thermal boundary layer at the base of the mantle may lie above its eutectic temperature. Such a partially molten zone would be expected to have enhanced thermal and chemical transport properties and may provide constraints on the geotherm and lateral variations in lowermost mantle temperature or mineralogy.

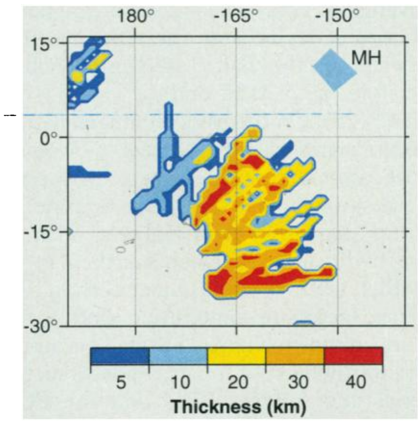

Fig. 1. Map view of the inferred thickness of the low-velocity anomaly, as constrained by $SP_{diff}KS$ ray results. Because the energy of diffracted *P* waves along the CMB is constrained to lie predominantly in the lowermost 50 km of the mantle, the thickness of this feature may be estimated from a combination of the observed time of arrival and length of travel of this phase along the CMB and waveform analyses [(*1*)]. MH denotes the location of the anomaly characterized by Mori and Helmberger using precursors to the reflected *PcP* phase (*2*).

Recent seismic observations show that the base of Earth's mantle has anomalously slow *P*-wave velocities (*1*, *2*). Evidence for a discrete layer is provided by two independent data types: (i) *SKS* waves that couple with short segments of core-diffracted *P* waves (*1*) and (ii) precursors to the core-reflected *PcP* phase (*2*). This layer is within the thermal boundary between the mantle and the core; depending on its origin, it may strongly influence the geomagnetic field, and it likely affected the evolution and differentiation of the deep Earth. The *P*-wave velocity in this layer is reduced by at least 10% relative to that in the mantle, with its thickness varying between ~5 and 40 km (*1*). Seismological data also imply that the transition between the basal layer and the overlying mantle is (at least locally) sharp [less than 10 km wide (*2*)]. The layer is thick beneath a region where the lower mantle has large-scale slower-than-average velocities (such as the central Pacific: Fig. 1) and is undetectable below average or faster-than-average lower mantle material (such as the circum-Pacific) (*1*), implying a relation with hot upwellings in the deep Earth.

Three phenomena could produce this anomalous basal layer: (i) partial melting, (ii) a chemical discontinuity, or (iii) a phase transition in mantle material near a pressure of 135 GPa, corresponding to depths just above the core-mantle boundary (CMB) (*3*). Although the first two possibilities are not exclusive, the last possibility is unlikely. Both Mg-rich silicate perovskite and $CaSiO_3$-perovskite appear to be stable at pressures spanning those present within most of the mantle (*4*, *5*); no significant phase transition is observed in (Mg,Fe)O in this pressure range (*6*), and the $CaCl_2$ structure of SiO_2 is apparently stable to pressures in excess of 130 GPa (*7*).

Thus, it appears that only a change in chemistry or the presence of melt can account for this reduction in seismic velocity. We first examined the possible origins of a change in melt fraction 40 km above the CMB. The amount of melt that can produce a 10% decrease in *P*-wave velocity may be estimated from the limited data set on elastic properties of silicate melts and their pressure dependence (*8*, *9*), coupled with treatments of the elastic behavior of two-phase aggregates (*10*, *11*). An upper bound on the effect of an Fe-rich fluid intercalated in the lowermost mantle may be derived if one assumes that the fluid has the properties of the outer core. If the fluid is instead an ultramafic silicate melt, its bulk modulus (*K*) under CMB conditions is uncertain but is likely to lie close to that of the solid mantle at these depths (*8*). Coincidentally, the *K* of core fluid is also close to that of the solid mantle at the CMB [644 GPa versus 653 GPa (*12*)]. We assumed that the *K* of the melt is equivalent to that of coexisting solid silicate mantle material. To estimate the size of the velocity change associated with the presence of partial melt, we also inferred the aggregate density. The density change associated with the melting of silicates at high pressures is

Earth Sciences Board and Institute of Tectonics, University of California, Santa Cruz, CA 95064, USA.

*To whom correspondence should be addressed.

likely to be small [order, 1% (*13*)] and will thus produce only small variations in the inferred velocities.

The amount of liquid necessary to generate a velocity change depends on the fluid geometry in the solid-liquid aggregate. If the liquid is present in either needle-like or spherical inclusions (*10*), a 25 to 30% volume fraction of fluid is necessary to generate a 10% reduction in *P*-wave velocity (Fig. 2). For comparison, films of melt are more effective in reducing seismic velocities; film aspect ratios control the amount of velocity depression (*11*). For aspect ratios of 0.01, melt fractions of as little as 5% could account for the observed shift in velocity (Fig. 2); smaller aspect ratios further reduce the necessary melt fraction. Thus, <5 to 30% melt can account for this layer: uncertainties in melt texture produce most of this variation.

The textural distribution of any fluid at the CMB must depend on its composition, which is difficult to assess solely on the basis of seismic data and modeling of partially molten aggregates. The primary distinguishing factor between a silicate melt and an Fe-rich liquid is their relative densities; both have similar bulk moduli at CMB conditions. Because of the higher density of an Fe-rich liquid, only about 20% intercalated melt of core chemistry can produce this velocity anomaly if the liquid is present in tubules or spheres. However, there have been suggestions that, in contrast to its behavior at lower pressure, liquid Fe may wet grain boundaries of silicates at high pressures (*14, 15*). If an Fe-rich fluid were present in grain-boundary wetting films with aspect ratios near 0.01, the small volume fraction of liquid (and thus a reduced effect on density) would produce an inferred liquid fraction similar to that of a silicate. However, the primary difficulty associated with an Fe-rich (or core-like) fluid may be dynamical in character: the high density, probable low viscosity, and likely wetting behavior (*14*) will probably cause such a liquid to descend into the outer core.

If partial melting does produce this anomaly, the magnitude of *S*-wave velocity perturbations within this zone should be diagnostic. Anomalies in *S*-wave velocity are roughly independent of melt geometries and would correspond to ~30% decreases (Fig. 3) for the inferred melt fractions of Fig. 2. Both seismic data sets used to image the low-velocity basal layer depend on *P*-wave velocity structure (*1, 2*); characterizing the magnitude of the shear velocity reduction depends on analysis of waveforms sensitive to *S*-wave velocity structure at these depths, such as the core-reflected *ScP* phase.

It is likely that chemical reactions such as

$$\begin{aligned}(Mg_xFe_{1-x})SiO_3 + 3[(1-x)-s]Fe \\ = xMgSiO_3 + [(1-x)-s]FeSi + sSiO_2 \\ + [3(1-x)-2s]FeO \qquad (1)\end{aligned}$$

occur at the CMB (*16*). Here, x is related to the amount of Fe present in reacting mantle material, and s is the amount of SiO_2 generated by the reaction. By volume, we expect from Eq. 1 that the first 4% of intruding core fluid will react with perovskite to form Fe-depleted silicate reaction products, with coexisting FeO and FeSi. It has been proposed that reaction products that are dominated by an Fe-depleted silicate perovskite have higher seismic velocities than the unreacted assemblage, with intruding (and reacting) Fe fluid initially augmenting seismic velocities (*15*). We estimated shifts in *P*-wave velocity for solid reaction products relative to reactants of differing Fe and Si contents (Fig. 4) by (i) using known elastic data for the phases in Eq. 1 (*17*), (ii) assuming that Poisson's ratio is constant from ambient conditions to those of the CMB, and (iii) calculating the relative velocity anomaly associated with CMB reactions for different amounts of added Fe (*18*). For plausible lower-mantle chemistries, the effect of such reactions on velocity (a maximum of 3 to 4%, with broad uncertainties) is smaller than the minimum 10% velocity depression needed to account for the seismic observations.

A chemical effect that could generate this feature without the presence of liquid is the presence of solidified core or Fe-rich alloy in this region; such material should have a lower seismic velocity than normal mantle. The amount of such material required to produce this anomaly hinges critically on the value of the shear modulus of core alloy at the CMB. Using a probable upper bound of 170 GPa for the shear modulus of Fe under these conditions [derived from the difference between the estimated bulk sound velocity and observed sound velocity of solid Fe at 135 GPa (*19*)], we estimate that an upper bound of 70 to 75% solidified core alloy could produce this velocity anomaly. However, if core material just above the CMB is close to its liquidus, the shear modulus could be small and the actual amount of solid alloy that could generate this anomaly would lie between this upper bound and our inferred possible abundance of core fluid of ~20%. Such entrainment of solid core material in the lowermost mantle would imply either (i) that a complex velocity structure is found in this layer, with entrained core material liquefying as the CMB is approached,

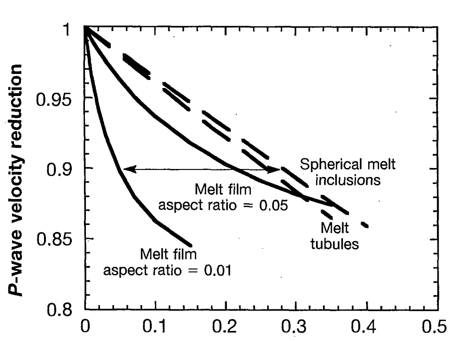

Fig. 2. The ratio of the *P*-wave velocity of melt-bearing mantle to that of solid mantle for varying melt fractions and melt geometries. The arrow indicates the range of melt fractions that produce a 10% *P*-wave velocity depression.

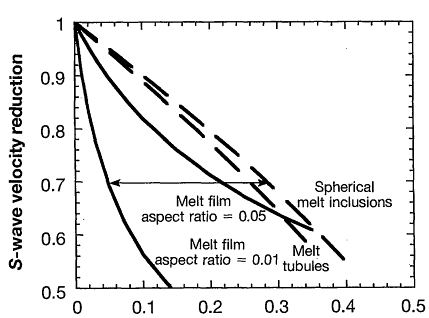

Fig. 3. The ratio of the *S*-wave velocity of melt-bearing mantle to that of solid mantle for varying melt fractions and melt geometries. The arrow corresponds to the variation in melt fraction implied by the inferred *P*-wave velocity depression of 10% coupled with the results in Fig. 2.

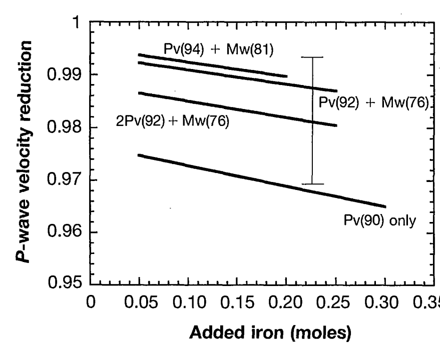

Fig. 4. Ratio of the *P*-wave velocity for assemblages that have undergone chemical reactions with variable amounts of Fe to that of the unreacted assemblage. The mole percent of Mg in perovskite (Pv) and magnesiowüstite (Mw) in the different unreacted assemblages are given in parentheses, and we derived the Fe/Mg ratios of these phases using the Fe-Mg partition coefficients of (*22*). The differing lengths of the lines is an indication of the maximum amount of Fe that can chemically react with the different assemblages, as given by Eq. 1. Because perovskite volumetrically dominates both the reacted and unreacted assemblages and no compositional dependence of the elastic properties (other than density) of perovskite has been observed (*4, 5*), the primary error in this ratio is produced by uncertainties in the elastic properties of FeO, FeSi, and SiO_2; the error bar reflects uncertainties in the bulk moduli and densities of these phases under CMB conditions.

or (ii) that the top of the outer core is close to its liquidus. The former possibility is difficult to assess, although observations of seismic wave scattering (*20*), as well as Fig. 1, document the region's complexity. The latter alternative is unlikely (unless there is either a significant thermal boundary at the top side of the core or suspended solids throughout the outer core) because the outer core adiabat is shallower than the liquidus of the core alloy (*21*).

If this low-velocity layer is produced by melting, then the most plausible means for generating an abrupt onset of the partially molten zone is if the geotherm intersects the eutectic temperature of the mantle. To generate up to 30% partial melting, the eutectic could lie neither near the mantle composition at these depths nor near the composition of silicate perovskite (probably the most abundant phase under these conditions) because significantly higher melt fractions would result. With this amount of melting, magnesiowüstite could lie near the eutectic and melt out of the solid assemblage over a narrow depth interval. Thus, the amplitude of this feature could produce a constraint on the mineralogy of the deep mantle; however, the topology of the multicomponent phase diagram of the mantle under CMB conditions is poorly constrained.

If this velocity anomaly is produced by the intersection of the geotherm with the solidus of silicate mantle material, then we would anticipate that this feature would be global in character but varying in its thickness, with lateral variations of the geotherm in the lowermost mantle. It is possible that, outside of the central Pacific and beneath part of the Atlantic (*1*), such a layer could be less than a few kilometers thick, rendering it difficult to image seismically. Because the outer surface of the core is essentially isothermal, it is possible that the topography of this basal layer could be produced by variable thermal gradients in the lowermost mantle, with thickening produced by local elevation of isotherms. The existence of such a partially molten layer should profoundly decrease the viscosity of the lowermost mantle, thus altering the heat transport out of the core, the stability of the thermal boundary layer at the base of the mantle, and potentially the flow regime in the lower mantle. Moreover, a partially molten layer is likely to have a higher electrical conductivity than unmelted mantle; this property could complicate the propagation of the geomagnetic field through this region of the planet.

REFERENCES AND NOTES

1. E. Garnero and D. V. Helmberger, *Phys. Earth Planet. Int.* **91**, 161 (1995); *Geophys. Res. Lett.* **23**, 977 (1996); E. Garnero, S. Grand, D. V. Helmberger, *ibid.* **20**, 1843 (1993). A velocity depression of at least 10% associated with this feature is derived from two-dimensional synthetic modeling of $SP_{diff}KS$ waveforms and delays (relative to *SKS*). Because $SP_{diff}KS$ data have very short (100 to 200 km) P_{diff} segments, these data help in providing an upper bound on the layer's thickness (40 km in the thickest regions). The trade-off between models having more extreme velocity reductions (within a thinner layer) and our preferred structure is greatly reduced by analysis of different data types (long- and short-period $SP_{diff}KS$ and short-period *PcP* precursors) over extended distance ranges.
2. J. Mori and D. V. Helmberger, *J. Geophys. Res.* **100**, 20359 (1995).
3. Anisotropy is precluded from playing a primary role in the origin of this feature, because no splitting is observed in either the $SP_{diff}KS$ phase (*1*) or the short-period *PcP* phase (*2*). Because the P_{diff} motion is parallel to the CMB, only azimuthal anisotropy would affect P_{diff}, and an azimuthally dependent splitting of $SP_{diff}KS$ arrivals should be produced by anisotropy. Furthermore, lowermost mantle anisotropy has been observed only for *S* waves [L. Vinnik, B. Romanowicz, Y. Le Stunff, L. Makeyeva, *Geophys. Res. Lett.* **22**, 1657 (1995)]; because *SKS* and $SP_{diff}KS$ waves travel nearly identical mantle paths, no differential effect of shear-wave anisotropy on these phases is expected.
4. E. Knittle and R. Jeanloz, *Science* **235**, 668 (1987).
5. H. K. Mao *et al.*, *J. Geophys. Res.* **96**, 8069 (1991).
6. M. Vassiliou and T. J. Ahrens, *Geophys. Res. Lett.* **9**, 127 (1982).
7. Y. Tsuchida and T. Yagi, *Nature* **347**, 267 (1990); K. Kingma, R. E. Cohen, R. J. Hemley, H. K. Mao, *ibid.* **374**, 243 (1995). Also, free SiO_2 is unlikely to be present in mantle assemblages that have not undergone reactions with core material (*16*).
8. A simple extrapolation of the estimated low-pressure bulk moduli (*K*) of ultramafic melts derived from ultrasonic measurements [M. L. Rivers and I. S. E. Carmichael, *J. Geophys. Res.* **92**, 9247 (1987); R. A. Secco, M. H. Manghnani, T. C. Liu, *Geophys. Res. Lett.* **18**, 1397 (1991)] with a zero-pressure dK/dP (K') of 6.8 (*23*) and a third-order Birch-Murnaghan equation of state (*7*) yields a *K* at the pressure of the CMB conditions of about 605 GPa. If the liquidus phase of mantle material is magnesiowüstite under these conditions (which it is to pressures of ~50 GPa), then the melt is likely to be enriched in SiO_2 relative to its residual solids [Q. Williams, *Geophys. Res. Lett.* **17**, 635 (1990); E. Ito and T. Katsura, in *High Pressure Research in Earth and Planetary Sciences*, M. Manghnani and Y. Syono, Eds. (American Geophysical Union, Washington, DC, 1992), pp. 315–322]. Under these conditions, increased SiO_2 content increases the average *K* of silicate liquids, whereas more magnesian melts are likely to be more compressible (*23*). Therefore, we consider that such estimates of the elasticity of the melt may provide a lower bound on the true value of *K*. As the *K* of the solid mantle at CMB conditions in the Preliminary Reference Earth Model model is about 653 GPa (*12*), we treat the *K* of the liquid as equivalent to that of the mantle at these depths. Our simulations are not particularly sensitive to this assumption.
9. F. Birch, *J. Geophys. Res.* **83**, 1257 (1978).
10. J. P. Watt, G. F. Davies, R. J. O'Connell, *Rev. Geophys. Space Phys.* **14**, 541 (1976).
11. J. B. Walsh, *J. Geophys. Res.* **74**, 4333 (1969).
12. A. M. Dziewonski and D. L. Anderson, *Phys. Earth Planet. Inter.* **25**, 297 (1981).
13. J. M. Brown, M. D. Furnish, R. G. McQueen, in *High Pressure Research in Mineral Physics*, M. Manghnani and Y. Syono, Eds. (American Geophysical Union, Washington, DC, 1987), pp. 373–384; S. M. Rigden, T. J. Ahrens, E. M. Stolper, *Science* **226**, 1071 (1984). The relative density of the liquid will also be increased if Fe partitions into the melt relative to coexisting solids, as it does to pressures of 25 GPa [C. Herzberg and J. Zhang, *J. Geophys. Res.* **101**, 8271 (1996)]. The small changes in volume observed on melting of silicates under shock loading, coupled with possible Fe enrichment of the liquid, are consistent with neutrally or negatively buoyant silicate liquids under deep mantle conditions.
14. S. Urukawa, M. Kato, M. Kumazawa, in *High Pressure Research in Mineral Physics*, M. Manghnani and Y. Syono, Eds. (American Geophysical Union, Washington, DC, 1987), pp. 95–111; W. G. Minarik, F. J. Ryerson, E. B. Watson, *Science* **272**, 530 (1996).
15. J. P. Poirier, *J. Geomagn. Geoelectr.* **45**, 1221 (1993).
16. E. Knittle and R. Jeanloz, *Science* **251**, 1438 (1991).
17. The Birch-Murnaghan equation of state is used to extrapolate densities and bulk moduli to conditions of the CMB (*9*). Because we assumed that Poisson's ratio is constant with compression, the bulk modulus, its pressure derivative, and Poisson's ratio are sufficient to calculate the high-pressure elastic properties of these assemblages. We used the zero-pressure *K* of perovskite and its pressure derivative from (*4*) and the zero-pressure shear modulus of this phase from A. Yeganeh-Haeri [*Phys. Earth Planet. Int.* **87**, 111 (1994)]. We assumed that substituted Fe has no effect on either the bulk or the shear modulus of perovskite; if added Fe lowers the shear modulus, as it does for most other oxides, then our calculated velocity depressions for CMB reactions are overestimated (*24*). The *K* of FeSi and its pressure derivative are from E. Knittle and Q. Williams [*Geophys. Res. Lett.* **22**, 445 (1995)], and the shear modulus is from J. L. Sarrao *et al.* [*Physica B* **199**, 478 (1995)]. The high-pressure phase of FeO is the only phase for which the shear modulus, and thus Poisson's ratio, is unconstrained: we used a zero-pressure, ambient-temperature *K* of 185 (±19) GPa, corrected for the 900 *K* value of Y. Fei and H.-K. Mao [*Science* **266**, 1678 (1994)], using an estimated zero-pressure temperature derivative of the bulk modulus of 2.2 (±0.8) × 10^{-2} GPa/K. Both this value for dK/dT and our assumed Poisson's ratio of 0.30 for the high-pressure phase of FeO are in general accord with that observed for a range of Fe-rich compounds (*24*). Elastic parameters for (Mg,Fe)O are from the compilation of Bass (*24*), and we assumed that the elastic moduli and density vary linearly with Fe content in this solid solution. For initial assemblages that incorporate magnesiowüstite, we assumed that any silica generated in Eq. 1 reacts with (Mg,Fe)O to form perovskite and that the generation of the high-pressure phase of FeO in Eq. 1 will produce a pure MgO phase coexisting with the high-pressure phase of FeO. Our velocity depressions are calculated with the use of a Voigt average over a perovskite (±magnesiowüstite) assemblage versus that for an Fe-free perovskite coexisting with an iron oxide, iron silicide, and either SiO_2-bearing or, if magnesiowüstite was initially present, perovskite-enriched phase assemblage (see Eq. 1).
18. Our calculation is not corrected for the effect of temperature; because we are calculating percentage changes in velocity, temperature will only alter the results of Fig. 4 if the temperature derivatives of the elastic properties of the assemblages in Eq. 1 are different under CMB conditions. However, the temperature derivatives of both the elastic moduli and their pressure derivatives are likely to be small under CMB conditions [T. S. Duffy and T. J. Ahrens, *J. Geophys. Res.* **97**, 4503 (1992)].
19. J. M. Brown and R. G. McQueen, in *High Pressure Research in Geophysics*, S. Akimoto and M. Manghnani, Eds. (Reidel, Dordrecht, Netherlands, 1982), pp. 611–623.
20. K. Bataille, R. S. Wu, S. M. Flatte, *Pure Appl. Geophys.* **132**, 151 (1990); F. Kruger, M. Weber, F. Scherbaum, J. Schlittenhardt, *Geophys. J. Int.* **122**, 637 (1995).
21. Q. Williams and R. Jeanloz, *J. Geophys. Res.* **95**, 19299 (1990); R. Boehler, *Nature* **363**, 534 (1993).
22. F. Guyot, M. Madon, J. Peyronneau, J. P. Poirier, *Earth Planet. Sci. Lett.* **90**, 52 (1988).
23. S. M. Rigden, T. J. Ahrens, E. M. Stolper, *J. Geophys. Res.* **94**, 9508 (1989).
24. J. D. Bass, in *AGU Handbook of Physical Constants* (American Geophysical Union, Washington, DC, 1995), vol. 2, pp. 45–63.

25. We thank R. Jeanloz, T. Lay, and the reviewers for comments; R. Jeanloz, L. Kellogg, E. Knittle, and T. Lay for discussions. This research was supported by the National Science Foundation and the W. M. Keck Foundation. This is Institute of Tectonics contribution 303.

14 March 1996; accepted 16 July 1996